

Geometrical Models for Liquid Metals and Alloys

J. Blétry

Institut Laue Langevin, 156X Centre de Tri, 38042 Grenoble Cedex, France
and LTPCM, ENSEEG, Domaine Universitaire

Z. Naturforsch. **33a**, 327–343 (1978); received November 15, 1977*

The structure of monoatomic liquids in the static approximation is described by a soft sphere model and the corresponding equation of state is derived. This geometrical model is then extended to binary liquid or amorphous substitution alloys where both components have the same size. The structure of these alloys is shown to be determined by the first neighbour order parameter which is positive, negative or zero for segregated, ordered or disordered alloys respectively. The variations of the partial structure factors with concentration are presented for these three cases. Size effects are then studied by varying the ratio of atomic diameters. Many experimental results are shown to fit this simple framework.

Introduction

Advanced liquid metal theories try to deduce the structure from the pair potential interaction by an approximate treatment. This problem presupposes a good knowledge of the interatomic potential. In order to avoid this difficulty and by following a phenomenological approach in which potential effects are introduced into a given structure, we recently proposed a soft sphere model which fits satisfactorily the most recent structure factor determinations on a wide variety of liquid metals [1].

In this paper, we complete our previous results on monoatomic liquids and derive the corresponding equation of state. This ‘geometrical’ model is then extended to binary liquid or amorphous alloys with components of equal size. Their structure is shown to depend mainly on the first neighbour order parameter which is positive, negative or zero for segregated, ordered or disordered liquid alloys respectively. The variations of the partial structure factors with concentration in these three cases are presented. Size effects are then studied by varying the ratio of atomic diameters. Most experimental results on binary liquid or amorphous alloys are finally shown to fit this simple framework.

Monoatomic Liquids

1. Basic Relations

At a given instant of time a monoatomic liquid is characterized by its static pair distribution function $P(r)$ which is the probability per unit volume of finding an atom at a distance r from another one,

Reprint requests to Dr. J. Blétry, Institut Laue Langevin, 156X Centre de Tri, F-38042 Grenoble-Cedex. 38041 St. Martin d’Hères

* 1st Version July 22, 1977.

normalized so that it tends to unity as r approaches infinity. The corresponding static structure factor is given by:

$$A(K) = 1 + \varrho \int \exp\{i \vec{K} \vec{r}\} [P(r) - 1] d_3r$$

where $\varrho = N/V$ is the number of atoms per unit volume.

According to the Ornstein-Zernike relation, the small K limit of the structure factor is proportional to the mean square fluctuation of the number density or to the isothermal compressibility

$$\chi = -\frac{1}{V} \left(\frac{\partial V}{\partial p} \right)_{T, N} : \\ A(0) = \frac{\bar{N}^2 - \bar{N}^2}{\bar{N}} = \varrho k_B T \chi \quad (1)$$

where k_B is the Boltzmann constant and T the temperature.

2. Random Hard Sphere Networks (RHSN)

2.1. Coordination Number and large K Behaviour of the Structure Factor

A hard sphere fluid depends on two parameters: the sphere diameter d or the sphere volume $v_0 = \pi d^3/6$ and the packing fraction γ which is the ratio of the volume of N spheres to the corresponding fluid volume V :

$$\gamma = N v_0 / V = \varrho v_0 .$$

The first neighbour peak in the pair distribution function $P_d^{\text{HS}}(r)$ is represented by a δ function which is proportional to the mean number η_γ of spheres in close contact with one sphere:

$$\eta_\gamma = \varrho \int_0^{d+\epsilon} P_d^{\text{HS}}(r) d_3r = 12.7 \gamma \quad \text{with } \epsilon \ll d. \quad (2)$$



Dieses Werk wurde im Jahr 2013 vom Verlag Zeitschrift für Naturforschung in Zusammenarbeit mit der Max-Planck-Gesellschaft zur Förderung der Wissenschaften e.V. digitalisiert und unter folgender Lizenz veröffentlicht:
Creative Commons Namensnennung-Keine Bearbeitung 3.0 Deutschland Lizenz.

Zum 01.01.2015 ist eine Anpassung der Lizenzbedingungen (Entfall der Creative Commons Lizenzbedingung „Keine Bearbeitung“) beabsichtigt, um eine Nachnutzung auch im Rahmen zukünftiger wissenschaftlicher Nutzungsformen zu ermöglichen.

This work has been digitized and published in 2013 by Verlag Zeitschrift für Naturforschung in cooperation with the Max Planck Society for the Advancement of Science under a Creative Commons Attribution-NoDerivs 3.0 Germany License.

On 01.01.2015 it is planned to change the License Conditions (the removal of the Creative Commons License condition “no derivative works”). This is to allow reuse in the area of future scientific usage.

This first neighbour δ peak is responsible for the large K behaviour of the structure factor since:

$$\lim_{K \rightarrow \infty} A_{d\gamma}^{\text{HS}}(K) = 1 + \eta\gamma(\sin(Kd)/Kd)$$

2.2. Structure Factor First Peak

For $Kd \lesssim 5\pi$ the structure factor differs from its asymptotic form. Thus model calculations are needed in order to find the position K_1 of the first $A_{d\gamma}^{\text{HS}}(K)$ peak. Our model leads to:

$$K_1 \cong 7.64/d. \quad (3)$$

The value $K_1d \cong 7.64$ differs from the value 7.725 which corresponds to the maximum of the first neighbour term $\sin Kd/Kd$. Thus, the first $A_{d\gamma}^{\text{HS}}(K)$ peak cannot be only attributed to the first neighbour peak in $P_d(r)$. On the contrary and according to Guinier [2], K_1 is related to the overall atomic arrangement i.e. to the repetition of some distance which is proportional to the sphere diameter d and may be named a “pseudoperiod”.

2.3. Close Packed Random Hard Sphere Network (CPRN)

If spheres are randomly removed from a RHSN the pair distribution function does not change while the structure factor decreases linearly with γ , following the relation:

$$A_{d\gamma}^{\text{HS}}(K) = 1 + (\gamma/\gamma_0)[A_{d\gamma_0}^{\text{HS}}(K) - 1].$$

Conversely, when γ increases linearly up to the Bernal value [3]:

$$\gamma_c = 0.637 \quad (4)$$

the extrapolated value of $A(0)$ i.e. the number density fluctuations of the RHSN vanish. Therefore, holes with atomic size should be absent from Bernal RHSN which we call the close packed random network (CPRN). In the CPRN the mean volume offered to each sphere is minimum:

$$v_c = (v_0/\gamma_c) = 1.57 v_0 \quad (5)$$

and the close contact coordination number reaches its maximum value:

$$\eta_c \cong 8.1. \quad (6)$$

3. Soft Sphere Liquid

3.1. Basic Relations

According to our model [1], a real liquid metal may be represented by an assembly of Einstein oscillators which vibrate at frequency ν around the equilibrium positions of a CPRN with randomly distributed vacancies. The sphere diameter is de-

duced from the position K_1 of the structure factor first peak by relation (3) while the packing fraction, which is supposed to be smaller than γ_c is deduced from the specific mass μ by:

$$\gamma = v_0(\mu/m)$$

where m is the atomic mass. The number M of vacancies in the volume V is related to the packing fraction by equation:

$$\gamma/\gamma_c = N/(N+M).$$

The pair distribution function (P.D.F.) and the structure factor of such a liquid are given by:

$$\begin{aligned} P_d^{\text{SS}}(r) &= (4\pi\sigma^2)^{-3/2} \int P_d^{\text{HS}}(\vec{r} - \vec{r}') \exp(-r'^2/4\sigma^2) d_3r', \\ A_{d\gamma}^{\text{SS}}(K) &= 1 + \exp(-\sigma^2 K^2) [A_{d\gamma}^{\text{HS}}(K) - 1] \end{aligned}$$

where:

$$\sigma^2 = \frac{\hbar}{8\pi^2 m \nu} \coth\left(\frac{\hbar\nu}{2kT}\right)$$

and \hbar is the Planck constant. The broadening of the first neighbour peak in the P.D.F. is responsible for the damping of the structure factor oscillations at large K according to relation:

$$\lim_{K \rightarrow \infty} A_{d\gamma}^{\text{SS}}(K) = 1 + \eta\gamma \exp(-\sigma^2 K^2) \sin(Kd)/Kd. \quad (7)$$

Conversely, Eq. (7) allows the determination of the vibration frequency from the damping of the structure factor oscillations.

On the other hand, owing to the broadening of the first neighbour peak, another coordination number Z is often used whose definition is:

$$Z = 2\varrho \int_0^d P(r) d_3r.$$

This coordination number is larger than 8.1 since neighbours which were not in close contact in the original CPRN are now included in this definition. For most liquid metals near the melting point: $Z \cong 10$.

3.2. Equation of State

Integration of the Ornstein Zernike relation would lead to the equation of state, however, we follow a more significant approach due to P. Nozières. The free energy of the liquid is the sum of two contributions: the oscillator free energy [4]:

$$F_a = 3N \left\{ \frac{\hbar\nu}{2} + kT \ln \left[1 - \exp\left(\frac{-\hbar\nu}{kT}\right) \right] \right\} - N U_a$$

(where U_a is the zero oscillation energy)

and the vacancy free energy:

$$F_h = M U_h - k T \ln \left[\frac{(N+M)!}{N! M!} \right]$$

where U_h is the vacancy formation energy while the entropy term represents the number of arrangements of M holes on $N+M$ sites. Both U_a and U_h can be calculated if one assumes that only first neighbour pairs contribute to these energies. Since $\frac{1}{2} \left(Z \frac{N}{N+M} \right)$ is the mean number of first neighbour pairs per atom the total pair energy is:

$$\begin{aligned} U &= -N U_0 \frac{1}{2} Z \frac{N}{N+M} \\ &= -N \left(\frac{1}{2} Z U_0 \right) + M \frac{N}{N+M} \left(\frac{1}{2} Z U_0 \right) \end{aligned}$$

where $-U_0$ is the energy of one atomic pair. This approximation leads to a zero oscillation energy:

$$U_a = \frac{1}{2} Z U_0$$

while the hole formation energy is given by:

$$U_h = \frac{1}{2} Z U_0 \frac{N}{N+M} = U_a \frac{N}{N+M}$$

Remembering that $V = (N+M) v_c$ and assuming that U_0 and v are independent of the number density one obtains the equation of state:

$$\begin{aligned} p &= - \left(\frac{\partial F}{\partial V} \right)_{T,N} \\ &= \frac{k T}{v_c} \ln \left(\frac{1}{1 - \frac{N v_c}{V}} \right) - U_a v_c \left(\frac{N}{V} \right)^2. \quad (8) \end{aligned}$$

The same result has already been obtained [5] by Barker in his lattice theory of the liquid state. At low temperature, the isotherms exhibit two extrema with one liquid and one gaseous branch while, at high temperature, these isotherms are monotonic. The critical temperature is given by:

$$k T_c = (U_a/2) = (Z U_0/4).$$

In the case of rare gases, where measurements are available, the calculated T_c value is larger than the experimental one. This result is not surprising since the model becomes too crude at low density where the vibration frequency should depend strongly on the density. However, the discrepancy is less than in Barker model because the coordination number Z

is approximately equal to 10 instead of 12 which is the value of a close packed lattice used by Barker.

Simulation of Binary Liquid Alloys by Hard Sphere Aggregates

For the sake of simplicity vibrational effects are excluded from our binary alloy study. In practice, hard sphere mixtures should provide a good description of liquid alloys where atomic radii are known to be additive and the structure is dominated by local order phenomena.

A liquid hard sphere alloy can be simulated by a randomly oriented aggregate (or cluster) with volume V containing N_1 spheres of diameter d_1 and N_2 spheres of diameter d_2 . For a given packing algorithm, such an aggregate depends on three parameters:

- the sphere diameter ratio $\delta = d_2/d_1$,
- the atomic concentration of chemical species 1

$$c_1 = N_1/(N_1 + N_2) = N_1/N$$

(or $c_2 = N_2/N = 1 - c_1$)

and the total packing fraction:

$$\gamma = \frac{\pi}{6} \frac{N_1 d_1^3 + N_2 d_2^3}{V}.$$

The partial packing fractions of species 1 and 2 are deduced from γ , δ and c_1 by means of relations:

$$\gamma_1 = \frac{c_1}{c_1 + c_2 \delta^3} \gamma, \quad \gamma_2 = \frac{c_2 \delta^3}{c_1 + c_2 \delta^3} \gamma. \quad (9)$$

1. Geometrical Packing Algorithm

In order to study the structure variations of hard sphere mixtures with concentration, sphere diameter ratio and local order, 80 aggregates containing 5000 spheres have been built with the aid of the time saving computing techniques described in Ref. [1]. The following geometrical packing algorithm has been used: Starting from an initial triangular seed of three spheres in contact, each aggregate is grown by successive additions of new spheres in contact with three spheres 0, A and B of the already existing aggregate. The "central" particle 0 is randomly chosen in the cluster and the pair A, B of particles belongs to its close neighbourhood Ω_0 . The choice of the pair A, B among all pairs belonging to Ω_0 as well as the chemical nature of the new particle P depend on some chemical packing algorithm which

determines the local chemical order and will be specified in the next section. If d_0 , d_A , d_B and d_P are the diameters of spheres 0, A, B and P, the coordinates of P are easily calculated since it is situated at distances $\frac{1}{2}(d_0 + d_P)$, $\frac{1}{2}(d_A + d_P)$ and $\frac{1}{2}(d_B + d_P)$ from 0, A and B. If the new sphere P does not overlap any sphere of its close neighbourhood Ω_P it is integrated to the cluster. The process is then repeated by choosing other pairs A, B belonging to the neighbourhood of 0 until Ω_0 is full, in which case another central particle 0' is randomly chosen in the cluster and so on.

2. Chemical Packing Algorithms

In analogy with order phenomena in solid solutions, one may distinguish disordered liquid alloys where chemical species are randomly mixed, ordered liquid alloys where unlike atoms attract each other and segregated liquid alloys where like atoms attract each other. These three alloy classes have been simulated by means of simple chemical packing algorithms. In all these algorithms the chemical nature of a particle P is specified with the aid of a chemical index i_P which is equal to 1 or 2 if P belongs to species 1 or 2.

Disordered alloys have been simulated with the aid of a chemical packing algorithm R1 which is symmetric with respect to both chemical species. According to R1, the new particle P which is added to the growing cluster with actual concentration c_{1a} belongs to species 1 if $c_{1a} \leq c_1$ and to species 2 if $c_{1a} > c_1$. P is brought tangentially to the sphere 0 and to a randomly chosen pair A, B pertaining to Ω_0 *.

Special attention has been paid to ordered alloys which have been simulated with the aid of two chemical packing algorithms, namely 01 and 02.

According to algorithm 01, the new particle P belongs to species 1 if $c_{1a} \leq c_1$ and to species 2 if $c_{1a} > c_1$. It is brought tangentially to the sphere 0 and to a pair A–B pertaining to Ω_0 which is chosen so as to maximize the number of 1–2 contacts between 0, A, B and P, i.e. to make the sum of their chemical indices $i_0 + i_A + i_B + i_P$ as close as pos-

* A second algorithm R2 for disordered alloy generation has also been tested in which a random number W is first chosen in the interval [0.1] and the new particle P belongs to species 1 if $W \leq c_1$ or to species 2 if $W > c_1$. Within the precision of our calculations, this algorithm gives the same result as the first one because randomness is already present in the choice of 0, A and B.

sible to 6. This chemical packing algorithm is symmetric with respect to both chemical species.

According to algorithm 02, a pair A–B of particles is first randomly chosen in Ω_0 . If one of the three particles 0, A and B belongs to species 1, the new particle P belongs to species 2 while if 0, A and B belong to species 2, P belongs to species 1 if $c_{1a} \leq c_1$ and to species 2 if $c_{1a} > c_1$. As usual, P is then brought tangentially to the spheres 0, A and B. This new ordering rule is asymmetric with respect to chemical species since 1–1 contacts are forbidden. (It is obviously impossible to forbid 1–1 and 2–2 contacts at the same time, or to forbid 1–2 contacts.)

Segregated alloys have been simulated with the aid of the symmetric packing algorithm S. According to S, the chemical nature of the new particle P is still 1 if $c_{1a} < c_1$ and 2 if $c_{1a} > c_1$. It is brought tangentially to the sphere 0 and to a particle pair A–B pertaining to Ω_0 which is chosen so as to maximize the number of like contacts between 0, A, B and P, i.e. to make the sum of their chemical indices $i_0 + i_A + i_B + i_P$ as close as possible to 4 or 8.

3. c_1 and δ Variation Range

If symmetric algorithms are used (R1, 01, S) the variation of the alloy structure with concentration and sphere diameter ratio δ may be studied in the reduced intervals:

$$\begin{aligned} 0 \leq c_1 \leq 1, \quad \delta \geq 1 \\ \text{or} \quad 0 \leq c_1 \leq 0.5, \quad \delta > 0 \end{aligned}$$

since the following symmetry relations are fulfilled

$$\begin{aligned} P_{22}^{c_1 \delta}(r/d_2) &= P_{11}^{c_1' \delta'}(r/d_1'), \\ P_{12}^{c_1 \delta}(r/d_{12}) &= P_{12}^{c_1' \delta'}(r/d_{12}'), \\ \text{or} \quad A_{22}^{c_1 \delta}(K d_2) &= A_{11}^{c_1' \delta'}(K d_1'), \\ A_{12}^{c_1 \delta}(K d_{12}) &= A_{12}^{c_1' \delta'}(K d_{12}') \end{aligned} \quad (10)$$

where $c_1' = 1 - c_1$, $\delta' = 1/\delta$ and $d_{\alpha\beta} = \frac{1}{2}(d_\alpha + d_\beta)$. If the non symmetric order algorithm 02 is used, concentrations larger than $c_1^{\max}(\delta)$ cannot be reached. Table 1 shows that $c_1^{\max}(\delta)$ corresponds to a constant number of 2–2 contacts per atom 2: $\eta_{22}^{\min}(\delta) \cong 4$. Actually, η_{22}^{\min} is the minimum value of the 2–2 partial coordination number which is needed to build a continuous RHSN of spheres 2 with isolated atomic holes for the accommodation of non contacting spheres 1.

δ	0.80	0.87	0.95	1	1.05	1.15	1.20
$C_1^{\max}(\delta)$	0.220	0.246	0.272	0.287	0.315	0.356	0.396
$\eta_{22}^{\min}(\delta)$	3.94	3.92	3.94	4.01	3.92	3.96	4.02

In practice, the variations of the alloy structure have been studied with 10% concentration steps and for values of the atomic diameter ratio ($\delta = 0.8, 0.87, 0.95, 1, 1.05, 1.15, 1.25$) which cover most of the experimental range. Numerical values are available on demand.

4. Shape of the Aggregates

A spherical shape is given to the clusters by imposing the condition that the distance r_i between a particle and the center of the cluster must be less than:

$$r_i < \frac{d_1}{2} \left[\frac{N}{\gamma} (c_1 + c_2 \delta^3) \right]^{1/3} = r_{\max}.$$

Conversely, the cluster radius R is deduced from the mean distance of the particle to the center of the cluster according to relation:

$$R = \frac{4}{3} r_m = \frac{4}{3} \frac{1}{N} \sum_1^N r_i.$$

R may also be calculated from the mean square distance r_{ms} of the particles to the center of the cluster:

$$R'^2 = \frac{5}{3} r_{ms}^2 = \frac{5}{3} \frac{1}{N} \sum_1^N r_i^2.$$

The comparison between R and R' leads to the definition of a sphericity coefficient $\alpha = R'/R$ which should be equal to 1 for a perfectly spherical cluster. Departures from sphericity are characterized by the relative difference $(\alpha - 1)/\alpha$ which, for all our clusters, is less than 10^{-3} .

5. Partial Pair Distribution Functions

The partial pair distribution functions $P_{\alpha\beta}(r)$ are defined as the probability per unit volume of finding an α particle at a distance r from another β particle normalized in such a way that they tend to unity as r approaches infinity. These functions are deduced from the number $dN_{\alpha\beta}(r)$ of distinct $\alpha\beta$ atomic pairs in the cluster whose distance $r_{ij}^{\alpha\beta} = |\vec{r}_j^{\beta} - \vec{r}_i^{\alpha}|$ lies in the interval $r, r + dr$:

Table 1. Maximum concentration and minimum partial coordination number in ordered alloys obtained by algorithm 02.

$$dN_{\alpha\beta}(r) = c_{\alpha} c_{\beta} \varrho^2 (2 - \delta_{\alpha\beta}) S(r) P_{\alpha\beta}(r) dr \quad \text{for } r < 2R \quad (11)$$

where $\delta_{\alpha\beta}$ is the Kronecker function ($\delta_{\alpha\beta} = 0$ if $\alpha \neq \beta$ and $\delta_{\alpha\beta} = 1$ if $\alpha = \beta$), and

$$S(r) = \frac{1}{6} \pi^2 (2R - r)^2 (4R + r)^2$$

a geometrical factor due to the finite size of the spherical cluster.

6. Partial Coordination Numbers

Within a sphere of radius r , the mean number $Z_{\alpha\beta}(r)$ of β atoms surrounding an α one is given by:

$$Z_{\alpha\beta}(r) = \int_0^r P_{\alpha\beta}(u) 4\pi u^2 du (N/V) c_{\beta}$$

and the total number $Z_{\alpha}(r)$ of atoms surrounding an α one by:

$$Z_{\alpha}(r) = \sum_{\gamma} Z_{\alpha\gamma}(r).$$

In hard sphere mixtures, where first neighbour peaks are described by δ functions, it is useful to consider the mean numbers $\eta_{\alpha\beta}$ of β atoms in close contact with an α atom, or partial coordination numbers:

$$\eta_{\alpha\beta} = Z_{\alpha\beta}(d_{\alpha\beta} + \varepsilon) \quad (12)$$

where ε is very small with respect to $d_{\alpha\beta}$ ($\varepsilon = 0.05 d_1$ is practically equal to the step of our $P_{\alpha\beta}$ calculations).

The non diagonal partial coordination numbers fulfill the obvious relations:

$$\eta_{\alpha\beta} c_{\alpha} = \eta_{\beta\alpha} c_{\beta} \quad \text{for } \alpha \neq \beta. \quad (13)$$

The total number of close contact neighbours to an α atom are given by:

$$\eta_{\alpha} = \sum_{\gamma} \eta_{\alpha\gamma}. \quad (14)$$

7. Bhatia Thornton's Partial structure Factors

The coherent scattering cross-section of a liquid alloy $d\sigma/d\Omega$ may be expressed with the aid of several partial structure factor (P.S.F.) sets which are linear combinations of one another [6]. Each set

completely defines the alloy structure. However, the physical meaning of each set is different and it is preferable to chose the set according to the physical nature of the problem being studied.

In the case of binary alloys, where the set of independent scattering factors b_1 and b_2 may be replaced by the set:

$$\bar{b} = c_1 b_1 + c_2 b_2, \quad \Delta b = b_1 - b_2.$$

Bhatia and Thornton [7] have introduced a set of structure factors which are quite useful for the study of local order phenomena since they are associated with the different correlations between total number density and concentration. The cross-section is then expressed as:

$$d\sigma/d\Omega = \bar{b}^2 S_{NN} + 2c_1 \bar{b} \Delta b S_{Nc_1} + c_1 c_2 (\Delta b)^2 S_{c_1 c_1}.$$

$\bar{b}^2 S_{NN}$ is the cross section of the “total” liquid which one measures when both alloy components have the same scattering factors.

Bhatia and Thornton (B.T.) partial structure factors fulfill simple inequality relations arising from the fact that $d\sigma/d\Omega$ must be a positive quadratic form in \bar{b} and Δb :

$$\begin{aligned} S_{NN} &\geq 0, \quad S_{c_1 c_1} \geq 0, \\ S_{NN} S_{c_1 c_1} &\geq (c_1/c_2) S_{Nc_1}^2. \end{aligned} \quad (15)$$

S_{NN} , S_{Nc} and S_{Cc} may be calculated from their Debye sum expressions [6] or from the following integral representations:

$$\begin{aligned} S_{NN} &= 1 + \varrho \int (c_1^2 P_{11} + c_2^2 P_{22} + 2c_1 c_2 P_{12} - 1) e^{iKr} d_3 r, \\ S_{Nc_1} &= \varrho c_2 \int [c_1 P_{11} - c_2 P_{22} + (c_2 - c_1) P_{12}] e^{iKr} d_3 r, \\ S_{c_1 c_1} &= 1 + \varrho c_1 c_2 \int (P_{11} + P_{22} - 2P_{12}) e^{iKr} d_3 r. \end{aligned} \quad (16)$$

However, in both methods, the truncation at $r = 2R$ produces spurious oscillations for

$$K \lesssim 6/(d_1 + d_2).$$

Therefore the small K limits of the partial structure factors are not accessible by our calculations and must be deduced from the study of density and concentration fluctuations.

8. Other Sets of Partial Structure Factors

A second expression of the cross-section is given by [8]:

$$d\sigma/d\Omega = \sum_{\alpha\beta} b_{\alpha} b_{\beta} (c_{\alpha} c_{\beta})^{1/2} N_{\alpha\beta}(K).$$

The integral representation of the corresponding partial number (P.N.) structure factors is:

$$N_{\alpha\beta} = \delta_{\alpha\beta} + \varrho (c_{\alpha} c_{\beta})^{1/2} \int [P_{\alpha\beta} - 1] e^{iKr} d_3 r. \quad (17)$$

The diagonal term $b_{\alpha}^2 c_{\alpha} N_{\alpha\alpha}$ represents the cross-section of partial liquid α and must be positive. As K approaches infinity it tends to:

$$\lim_{K \rightarrow \infty} N_{\alpha\alpha} = 1 + \eta_{\alpha\alpha} \sin(K d_{\alpha})/K d_{\alpha}$$

except when $\eta_{\alpha\alpha} = 0$.

Fournet, Faber and Ziman [9], [10] (FFZ) give another expression for the coherent cross-section of a liquid alloy:

$$d\sigma/d\Omega$$

$$= \frac{1}{2} \sum_{\alpha\beta} c_{\alpha} c_{\beta} (b_{\alpha} - b_{\beta})^2 + \sum_{\alpha\beta} c_{\alpha} c_{\beta} b_{\alpha} b_{\beta} A_{\alpha\beta}(K).$$

The FFZ partial structure factors have the following integral expressions:

$$A_{\alpha\beta} = 1 + \varrho \int (P_{\alpha\beta} - 1) e^{iKr} d_3 r \quad (18)$$

which do not explicitly involve the concentrations. Therefore the concentration variations of the FFZ structure factors characterize the deviations from the ideal behaviour where the partial pair distribution functions are concentration independent. The diagonal FFZ structure factor $A_{\alpha\alpha}$ which is not proportional to any partial cross-section fulfills a complex inequality relation [11].

Substitution Alloys: $\delta = 1$

1. Relation Between Structure and Order Parameter ξ

The study of liquid alloys with components of equal size or substitution alloys, displays the effect of pure chemical ordering. In such cases, within our simple algorithms, both kinds of atoms have the same total number of neighbours for all pair distances:

$$Z_1(r) = Z_2(r)$$

and the partial pair distribution functions fulfill the following relations:

$$c_1 P_{11} + c_2 P_{12} = c_2 P_{22} + c_1 P_{21} = P_d(r) \quad (19)$$

where $P_d(r)$ is the pair distribution function of the pure hard sphere liquid with the same sphere diameter $d = d_1 = d_2$. Thus, there are only two independent partial pair distribution functions. Furthermore, the maximum packing fraction is the same as for pure liquids: $\gamma_c = 0.637$ and the co-

ordination numbers are related to γ by:

$$\eta_1 = \eta_2 = \eta_\gamma = 12.7 \gamma. \quad (20)$$

On the other hand, a statement equivalent to relation (19) is that there is no correlation between local number density and concentration since the permutation of an atom 1 by an atom 2 changes the local concentrations without changing the local densities. As a consequence, the use of B.T. formalism is particularly convenient in that case since:

$$S_{NN} = 1 + \varrho \int [P_d(r) - 1] e^{iKr} d_3 r = A_{d\gamma}^{\text{HS}}(K) \quad (21)$$

is independent of the local chemical order and equal to the structure factor of the pure liquid with the same packing fraction, while:

$$S_{NC} = 0 \quad (22)$$

and:

$$S_{CC} = 1 + \varrho c_1 \int [P_{11} - P_{12}] e^{iKr} d_3 r \quad (23)$$

completely defines the local chemical order.

Let us introduce the Bethe first neighbour order parameter [12] which has been used by Steeb and Hezel [13] in the analysis of their data on Mg-Ag alloys:

$$\xi = 1 - \frac{\eta_{12}}{\eta_1} \frac{1}{c_2} = 1 - \frac{n_{21}}{\eta_2} \frac{1}{c_1}. \quad (24)$$

The large K behaviour of S_{NN} and S_{CC} is particularly revealing since it only depends on n_γ and ξ through the asymptotic relations:

$$\lim_{K \rightarrow \infty} S_{NN} = 1 + \eta_\gamma [\sin(Kd)/Kd], \quad (25)$$

$$\lim_{K \rightarrow \infty} S_{CC} = 1 + \xi \eta_\gamma [\sin(Kd)/Kd]. \quad (26)$$

These asymptotic forms become fairly good approximations beyond $Kd \approx 5\pi$ but they do not hold below $Kd \approx 5\pi$. In particular, at smaller K values, the behaviour of S_{CC} is related to the overall atomic order and also depends on order parameters of more distant neighbours. However, the qualitative behaviour predicted by Eq. (25) is still valid for small K and S_{CC} superstructure oscillations increase with $|\xi|$ (see Figure 1). Inversely, knowing c_1 and the amplitude of S_{CC} first extrema which are not too sensitive to vibrational effects, it should be possible to calculate ξ and to derive the mean proportion of like to unlike atoms around each atom (see Table 2).

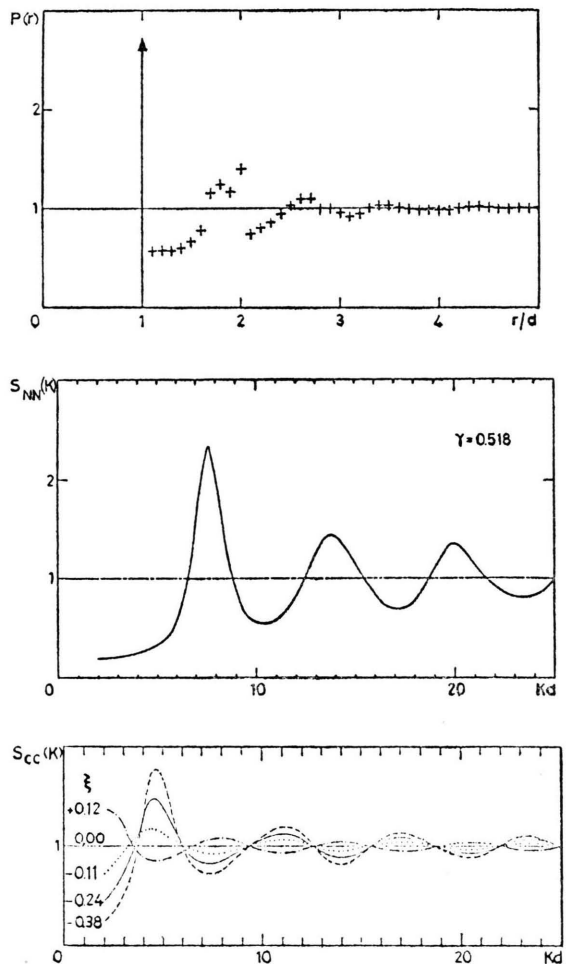


Fig. 1. Variations of B.T. structure factors with order parameter ξ in substitution alloys.

2. Disordered Alloys: $\xi = 0$

This is the simplest case where the presence of the second component introduces randomly distributed holes in the RHSN of the first component and vice versa. In these conditions, all three partial pair distribution functions are equal and concentration independent (see Figure 1):

$$P_{11} = P_{12} = P_{22} = P_d^{\text{HS}}(r)$$

and the partial coordination numbers are given by:

$$\begin{aligned} \eta_{11} &= \eta_{21} = c_1 \eta_\gamma, \\ \eta_{12} &= \eta_{22} = c_2 \eta_\gamma. \end{aligned} \quad (27)$$

As a consequence $\xi = 0$ and these alloys give rise to a constant Laue diffuse scattering $S_{CC} = 1$. The

Table 2. Variation of the first S_{NN} and S_{CC} extrema with ξ in substitution alloys ($\gamma = 0.518$).

Algorithm	02	02	02	01	S	S
C_1	0.10	0.20	0.287	0.5	0.3	0.5
η_{12}/η_1	1	1	1	0.694	0.644	0.441
ξ	-0.110	-0.236	-0.381	-0.391	0.120	0.116
$S_{NN}(K_1)-1$	1.268	1.68	1.245	1.268	1.230	1.235
$S_{CC}(K_S)-1$	0.182	0.476	0.784	0.869	-0.140	-0.159
$S_{CC}(K_1)-1$	-0.079	-0.181	-0.288	-0.279	0.077	0.093

associated FFZ partial structure factors are equal, positive and concentration independent:

$$A_{11} = A_{12} = A_{22} = A_{d\gamma}^{\text{HS}}(K).$$

This is the unique case where FFZ structure factors do not depend on concentration. Therefore the concentration method for partial structure factor determination is subject to the very restrictive conditions: $\delta = 1$, $\xi = 0$.

3. Ordered Alloys: $\xi < 0$

3.1. Common Properties

In ordered alloys obtained by algorithms 01 or 02, the presence of the second component introduces non randomly distributed atomic holes in the RHSN of the first component and vice-versa. As a consequence, the partial P.D.F. depend on concentration.

Since the behaviour of S_{NN} equally depends on all chemical pairs, it is not modified by atomic ordering. Thus the first S_{NN} peak at K_1 is still related to d through relation (3). On the other hand, in close analogy with the case of order phenomena in crystallized alloys, atomic ordering produces an overall repetition of a new distance d_s . This new pseudoperiod is related to the chemical packing algorithm, i.e. to the order parameters of the first few neighbours and gives rise to a sharp "superstructure" peak at

$$K_S = 0.612 K_1. \quad (28)$$

It turns out that d_s can be interpreted as the distance between two atomic "layers" belonging to the same chemical species separated by one atomic "layer" belonging to the other chemical species:

$$d_s = \frac{2\sqrt{2}}{\sqrt{3}} d = \frac{d}{0.612}.$$

On the other hand, at large K , S_{NN} and S_{CC} oscillate in phase opposition according to relations (25) and (26).

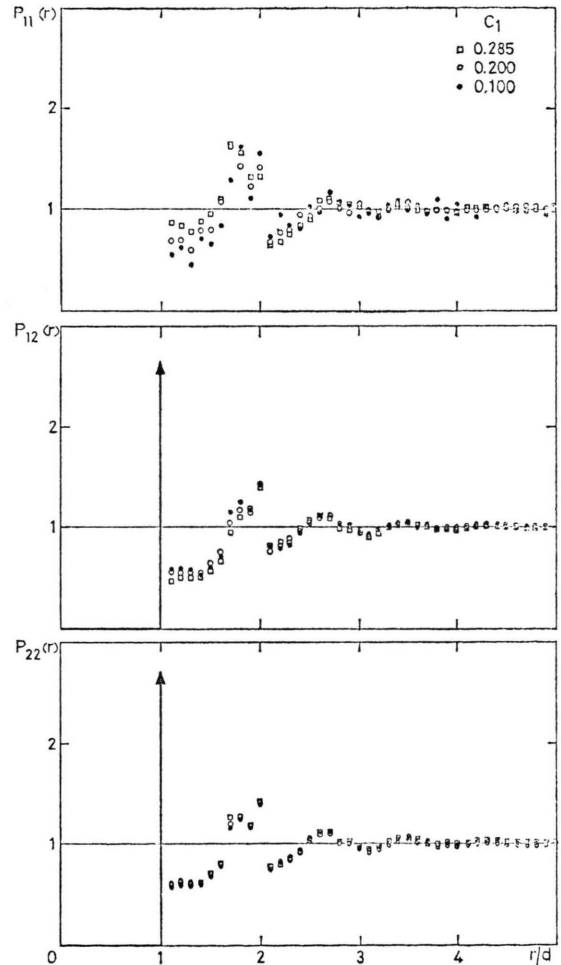


Fig. 2. Variations of partial pair distribution functions with concentration in ordered substitution alloys obtained by algorithm 02.

3.2. Maximum Order Alloys

In maximum order alloys where 1-1 contacts are forbidden, the main features of the partial P.D.F. are (see Figure 2):

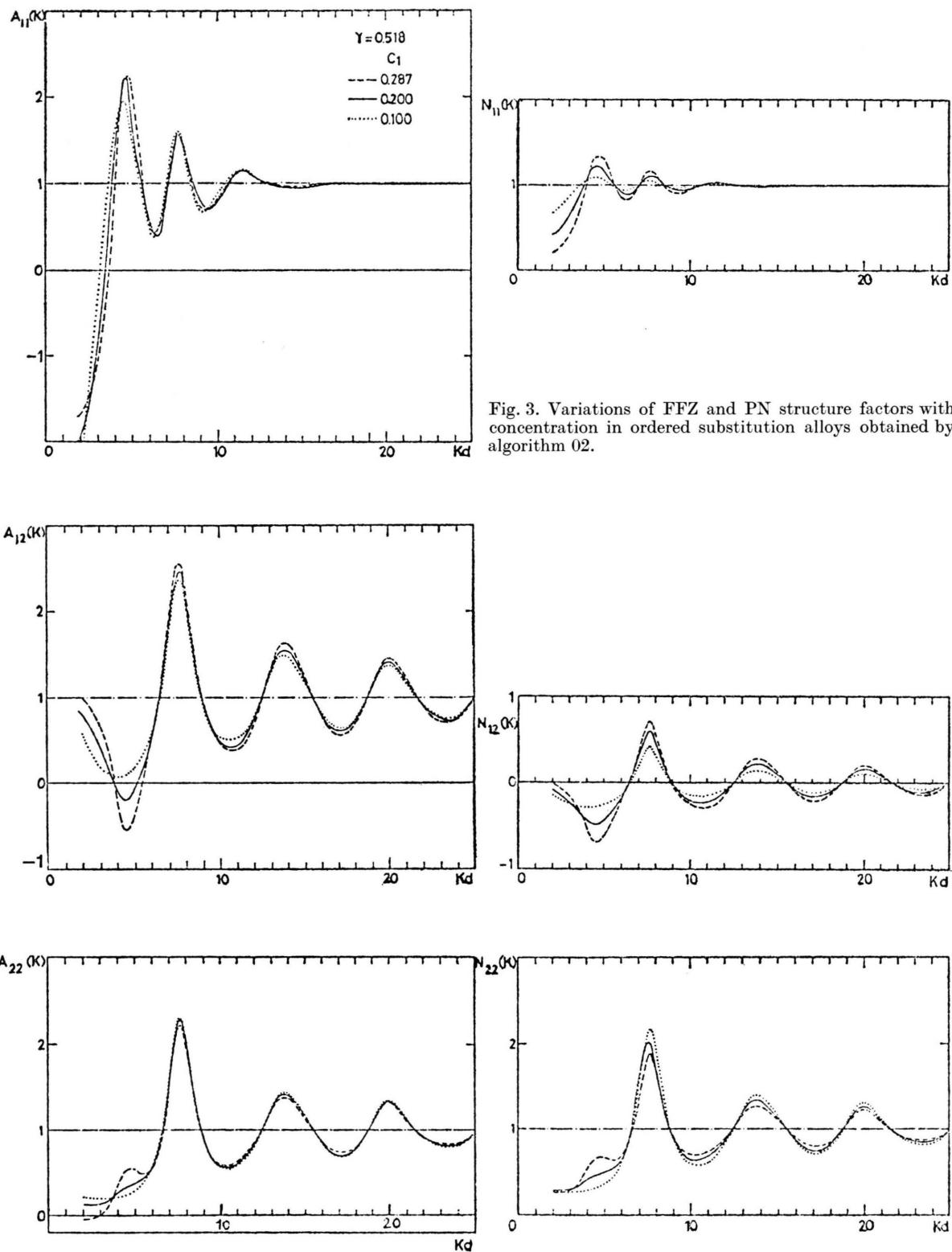


Fig. 3. Variations of FFZ and PN structure factors with concentration in ordered substitution alloys obtained by algorithm 02.

- i) the disappearance of the first neighbour delta peak in P_{11} corresponding to: $\eta_{11} = 0$ for all concentrations;
- ii) the finite width of the first P_{11} maximum which is the second neighbour peak;
- iii) the increase of the first neighbour delta peak in P_{12} corresponding to $\eta_{12} = \eta_1 = 12.7 \gamma$.

As a consequence in reciprocal space, A_{11} is almost concentration independent (i), tends to a large negative value at small K and displays a sharp superstructure peak at K_S (ii) together with strongly damped oscillations at large K (ii) (see Figure 3). This A_{11} behaviour has also been predicted by Laty et al. [14] in the dilute alloy limit. On the other hand, $A_{12}(K)$ tends to a positive value at small K and displays a superstructure dip at K_S together with increased oscillations at large K (iii) (see Figure 3). All these A_{12} features increase with concentration c_1 . $A_{22}(K)$ is almost concentration independent except for a superstructure bump at K_S whose height increases with c_1 (see Figure 3). This indirect effect is due to the regular array of holes introduced by the ordered component 1 in the RHSN of component 2.

In Figure 3, we have also plotted the variations of the P.N. structure factors with concentration. Their peak positions are obviously the same as for FFZ structure factors but N_{11} and N_{22} do not exhibit any negative part as anticipated in Part 8 of the last section.

4. Segregated Alloys: $\xi > 0$

The behaviour of these alloys, which correspond to $\xi > 0$, can be inferred from the behaviour of ordered alloys obtained by algorithm 01 by inverting the roles of like and unlike chemical pairs. Owing to the overall increase of the minimum distance between unlike atoms, S_{CC} exhibits a superstructure dip at $K_S = 7.64/d_S$ where d_S is the distance between two atomic layers belonging to different chemical species separated by one atomic layer. Consequently A_{11} and A_{22} tend to positive values at small K and display superstructure dips at K_S together with increased oscillations at large K while A_{12} exhibits a superstructure bump at K_S and reduced oscillations at large K (see Figure 4). This A_{11} behaviour has also been predicted by Laty et al. [14] in the dilute alloy limit.

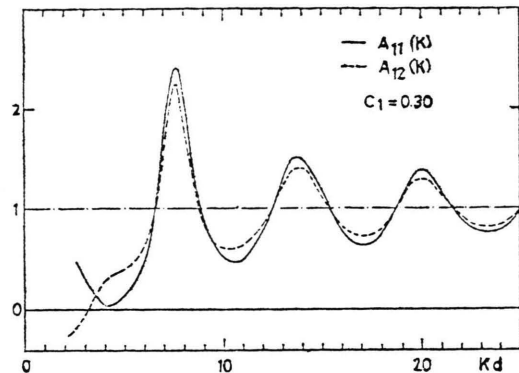


Fig. 4. FFZ structure factors of segregated substitution alloys.

Size Effects

When alloy components differ in atomic diameter, the maximum packing fraction may be larger than in a pure hard sphere liquid since holes smaller than atomic size in the RHSN of the larger spheres can be filled by the smallest spheres [3]. However, we do not concentrate on this problem and our calculations correspond to $\gamma = 0.535$.

1. Disordered Alloys

1.1. Coordination Numbers

The partial coordination numbers obviously depend on the maximum (integer) number $p(\delta)$ of spheres with diameter d_1 which can surround a sphere with diameter d_2 . $p(\delta)$ increases with δ following a step-like curve whose discontinuities are given by the approximate Fejes Tóth equation [15]:

$$\sin^2\left(\frac{p}{p-2} \frac{\pi}{6}\right) = \frac{(\delta+1)^2}{4\delta(\delta+2)}.$$

This equation is exact for $p = 3, 4, 6$ and 12 (i.e. for equilateral triangle, regular tetrahedra, octahedra and icosahedra) and when p approaches infinity i.e. when the surface of sphere 2 is almost plane and covered by an hexagonal lattice of spheres 1:

$$\lim_{\delta \rightarrow \infty} p = (2\pi/\sqrt{3})\delta^2.$$

Exact values of $p(\delta)$ discontinuities which are slightly larger than Tóth values (see Figure 5) have been calculated by Schütte [16]. A good approximation to the lower limit of the Schütte curve in the interval $0.5 < \delta < 1.5$ is the linear relation:

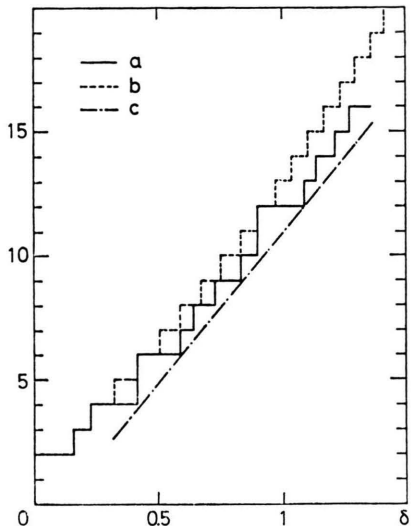


Fig. 5. Variations of the maximum number of close contact neighbours with the sphere diameter ratio

- a) Schütte and van den Waerden values [16],
- b) Fejes Tóth approximation [15],
- c) linear approximation (29).

$$p \cong 12\delta - 1 \quad (29)$$

where p is no more an integer (see Figure 5).

Thus it is natural to assume that the partial coordination numbers of disordered alloys are approximately equal to:

$$\eta_1 \cong \eta_\gamma \frac{d_1}{\bar{d}} = \frac{\eta_\gamma}{c_1 + c_2 \delta}, \quad \eta_2 \cong \eta_\gamma \frac{d_2}{\bar{d}} = \eta_\gamma \frac{\delta}{c_1 + c_2 \delta} \quad (30)$$

where $\bar{d} = c_1 d_1 + c_2 d_2$ is the mean sphere diameter. For $\gamma = 0.535$, numerical calculations confirm this assumption with a precision better than 0.5%.

However, the variations of coordination numbers η_{12} and η_{21} with concentration do not follow the

linear relations (27) (see Figure 6). Therefore it is difficult to define an order parameter which separates local chemical order effects from size effects.

1.2. Variation of Disordered Alloy Structure With Concentration and Sphere Diameter Ratio

In disordered alloys randomly distributed holes are introduced by component 2 in the RHSN of component 1 but their size differs from d_1 . As a consequence, the partial pair distribution functions depend on concentration and sphere diameter ratio. This dependence is mainly reflected in the first neighbour delta peaks of the partial P.D.F. through the partial coordination numbers $\eta_{\alpha\beta}$ studied in the last section. The other P_{11} oscillations shift towards larger r as δ increases from 1 upwards while the other P_{12} oscillations are less sensitive to δ variations (see Figure 7).

The corresponding FFZ structure factors do not exhibit any superstructure peak nor large negative part. However, their first peaks become more and more asymmetric and the oscillation damping more and more important as δ goes away from 1 (see Figure 8). The partial structure factor $A_{\alpha\alpha}$ of the smallest size component is obviously the most affected. Numerical calculations show that the positions $K_1^{\alpha\beta}$ of $A_{\alpha\beta}$ first maxima are approximately given by the phenomenological relation:

$$K_1^{\alpha\beta} = \frac{1}{d_{\alpha\beta}} \left[7.64 - 4.32 \left(\frac{\bar{d}}{d_{\alpha\beta}} - 1 \right) \right] \quad \text{for } 0.8 < \delta < 1.25. \quad (31)$$

Conversely, from the positions of the first peaks of the experimental P.S.F. one may calculate d_{11} , d_{12} and d_{22} and check the validity of the additivity law

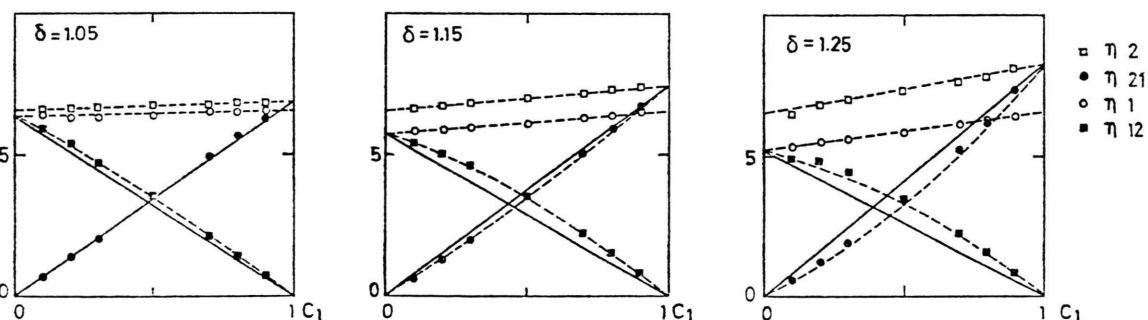


Fig. 6. Variations of the partial coordination numbers with concentration and sphere diameter ratio in disordered alloys.

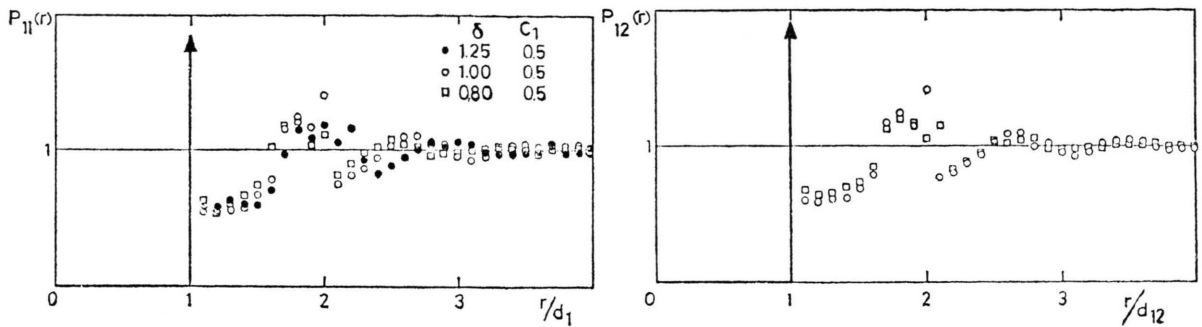


Fig. 7. Variations of the partial pair distribution functions with sphere diameter ratio in disordered alloys.

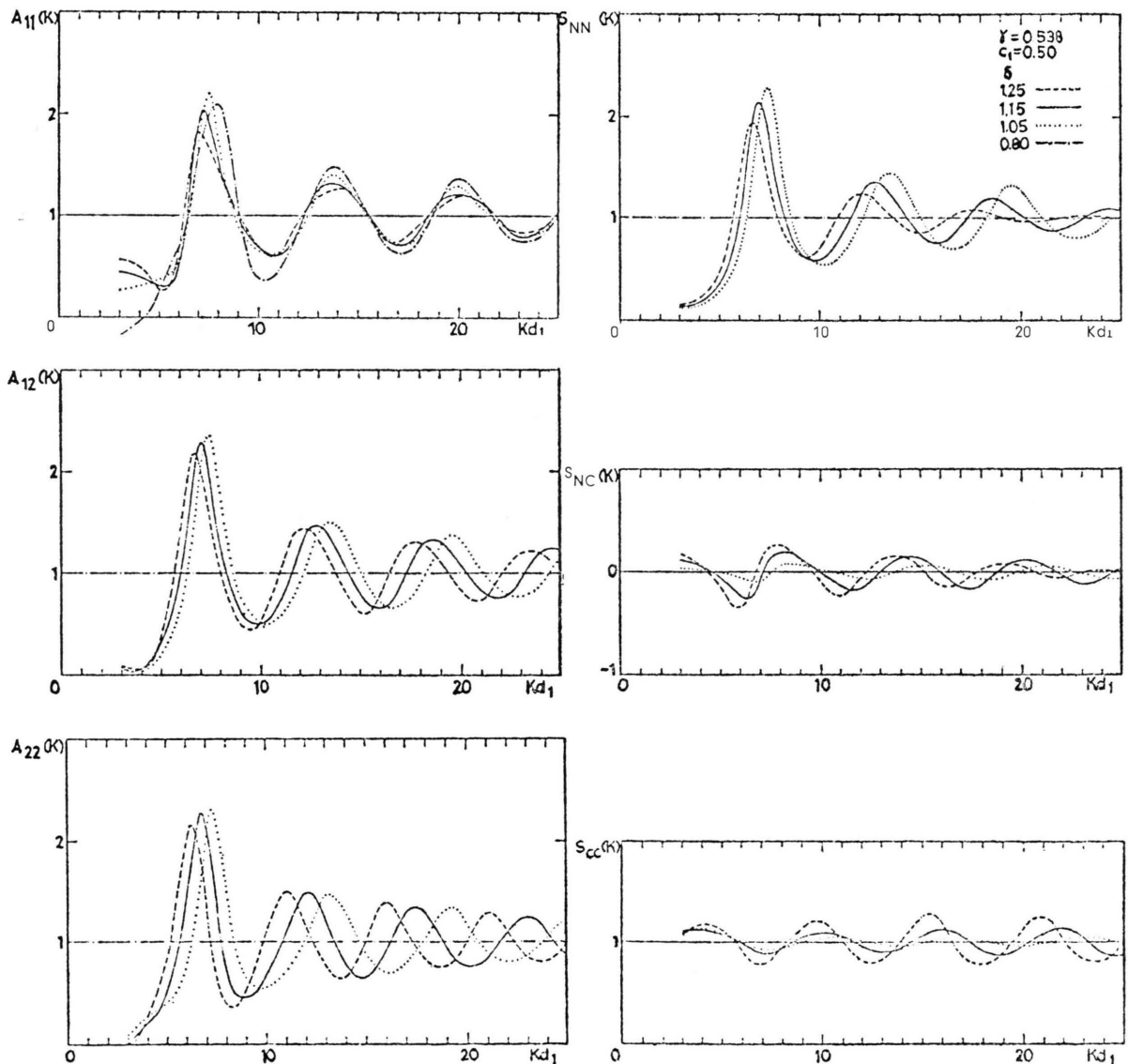


Fig. 8. Variations of FFZ and B.T. structure factors with sphere diameter ratio in disordered alloys.

for atomic diameters since d_{12} should be equal to $\frac{1}{2}(d_{11} + d_{22}) = \frac{1}{2}(d_1 + d_2)$.

On the other hand, S_{NC} "size oscillations" appear which are due to the correlation between number density and concentration. S_{NC} and S_{CC} size oscillations increase as δ goes away from 1. S_{NN} first peak is situated at:

$$K_1^{NN} = 7.64/\bar{d} \quad (32)$$

as might be expected (see Figure 8). According to relations (16) BT structure factors display beating oscillations at large K between three terms proportional to $\sin(Kd_1)/Kd_1$, $\sin(Kd_{12})/Kd_{12}$ and $\sin(Kd_2)/Kd_2$. This behaviour is usually masked by the oscillation damping due to atomic vibrations. Nevertheless, it can explain the long range of BT structure factor oscillations in disordered alloys.

2. Ordered Alloys

2.1. General Behaviour

The qualitative behaviour of ordered alloys with nonequal size components is the same as the one of ordered substitution alloys. Let us compare the BT structure factors of ordered alloys (obtained by algorithms 01 or 02) with the BT structure factors of disordered alloys corresponding to the same δ value. S_{NN} is almost insensitive to local chemical order and identical to S_{NN} of disordered alloys. In particular the position of its first peak is still given by Equation (32). On the other hand, the position of S_{NC} size oscillations is the same as in disordered alloys but their amplitude is smaller. The main difference with disordered alloys lies in the first S_{CC} superstructure peak whose relative position with respect to S_{NN} first peak is almost independent of δ and given by equation: $K_S \approx 0.61 K_1$. S_{CC} oscillations at larger K values are identical with those of disordered alloys (see Figure 10).

2.2. Variation of the Structure Factors of Maximum Order Alloys

Maximum order alloys obtained by algorithm 02 are characterized by the complete disappearance of the P_{11} first neighbour delta peak (see Figure 9). Consequently, A_{11} exhibits a large negative part at small K , a strong superstructure peak at $K_S(\delta)$ and is strongly damped at large K . In particular it only displays two oscillations if $\delta > 1$ and three oscillations if $\delta < 1$ (see Figure 10). On the other hand, A_{12} reaches positive values at small K and displays

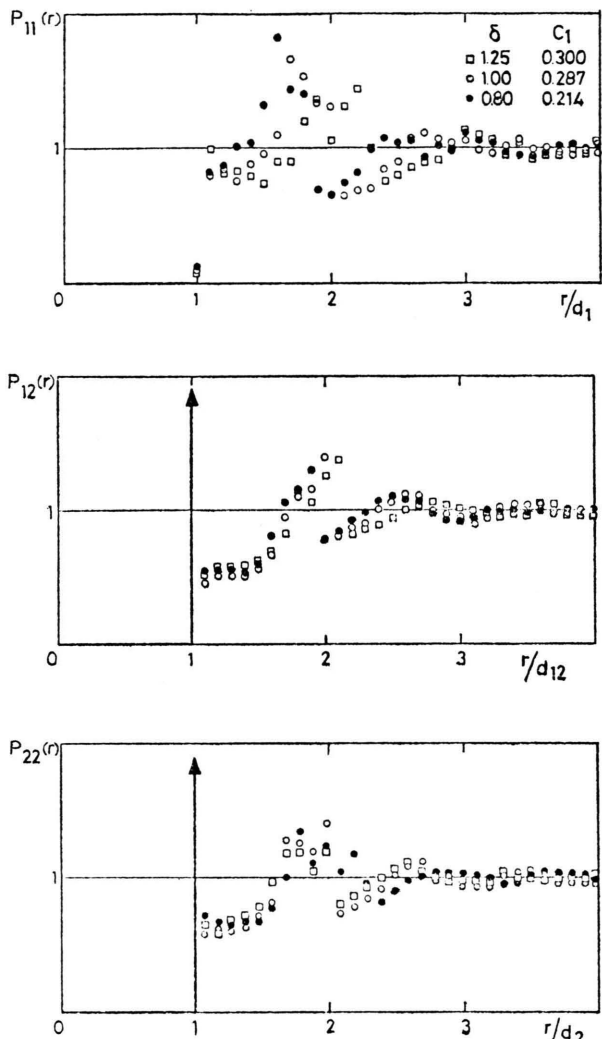


Fig. 9. Variations of the partial pair distribution functions with sphere diameter ratio in ordered alloys obtained by algorithm 02.

a negative superstructure dip at K_S and increased oscillations at large K . Finally, A_{22} only displays an "indirect" superstructure bump which may reduce to a slight asymmetry of the first peak if δ is larger than 1 (see Figure 10).

Comparison with Experiments

1. First Results

A direct comparison between calculated and measured PSF is preferable to a comparison between the corresponding PDF which requires a Fourier trans-

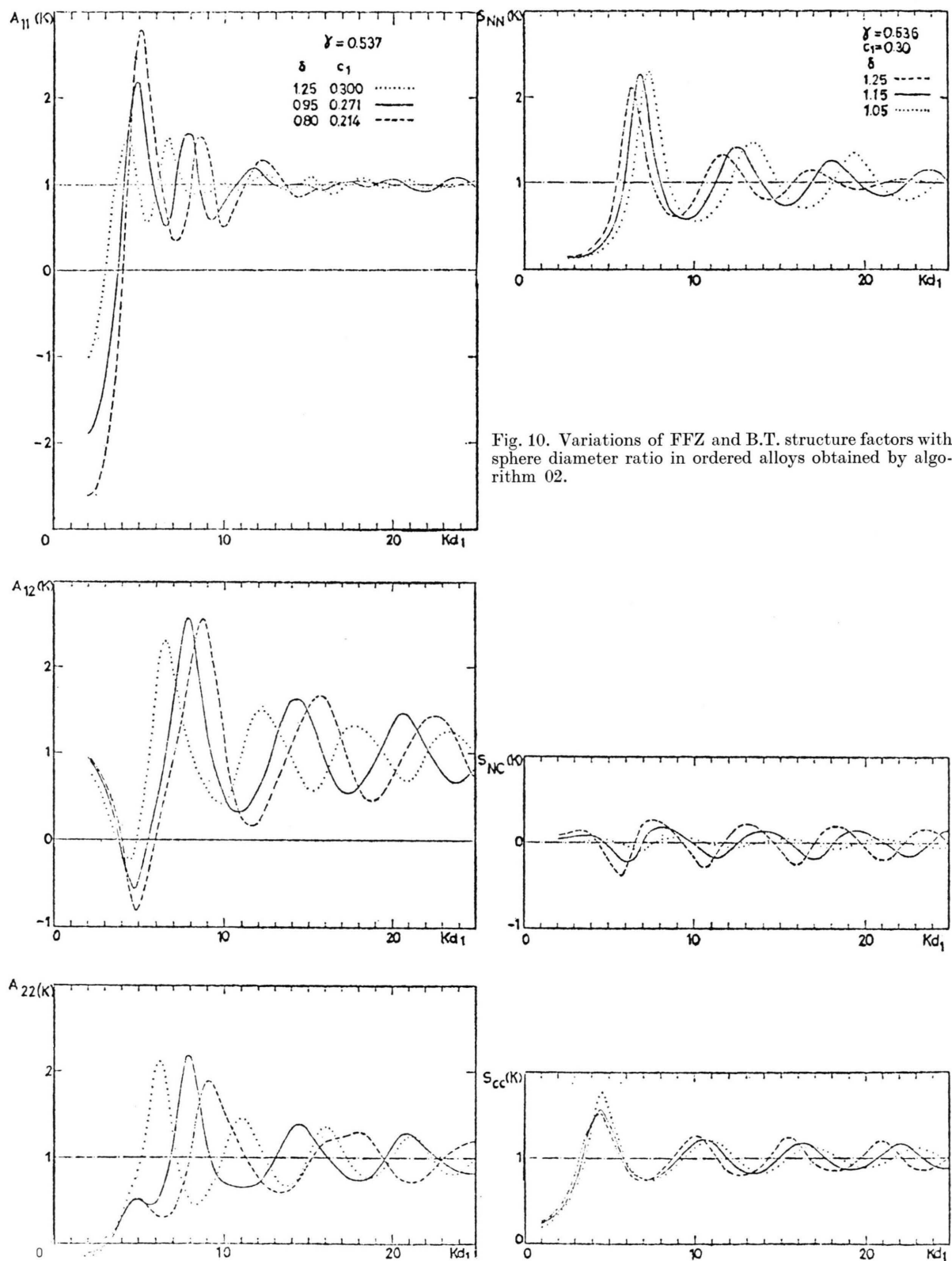


Fig. 10. Variations of FFZ and B.T. structure factors with sphere diameter ratio in ordered alloys obtained by algorithm 02.

form of the experimental data and is subject to truncation and normalization errors. Furthermore, conclusions may be drawn from the behaviour of the PSF in a limited K interval since local chemical order phenomena produce characteristic effects before the first PSF peaks and are damped by vibrational effects at large K .

The observation of prepeaks in the scattering patterns of liquid alloys has been shown to be related to order phenomena by Steeb et al. [13] as early as 1966 and many analogous studies have since been performed [17]–[22]. However, since model calculations show that partial structure factors usually depend on concentration, we treat in detail those later partial structure factor determinations which are not based on the assumption of concentration independency. Such a partial structure factor determination in binary alloys requires the measurement of three independent cross-sections corresponding to the same concentration and the resolution of a linear system of three equations in A_{11} , A_{12} and A_{22} [23]. This delicate procedure has been achieved in only a few particular cases.

2. Disordered Alloys

The first measurements not based on the assumption of concentration independency were performed by Enderby, North and Egelstaff [11] using the isotopic substitution method. Their results show that Cu₆-Sn₅ liquid alloys are disordered since the PSF do not exhibit any superstructure peak nor large values of $A_{ij}(0)$. Furthermore, Cu₆-Sn₅ partial structure factors exhibit large first peak asymmetries corresponding to a strong size effect. However, the atomic diameters which are deduced by relations (31) from the position of the PSF first peaks seem not to be additive. This result is confirmed by North and Wagner measurements on the same system [24]. It may be related to the 'anomalous' shoulder on the first peak of the pure tin structure factor which indicates a special liquid Sn structure or to a departure from sphericity of the interatomic Sn-Sn potential. It may also arise from covalency effects.

3. Ordered Alloys

In ordered alloys, partial structure factor determinations not based on the assumption of concentration independency have been reported by Blétry

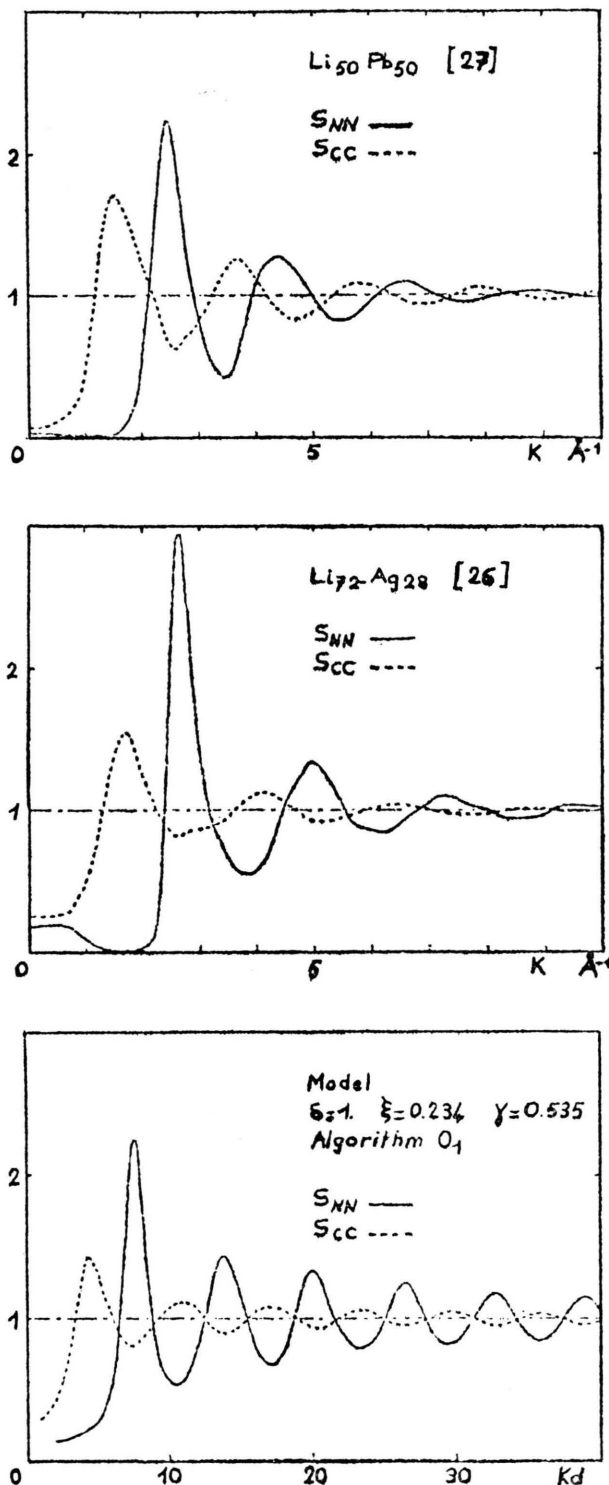


Fig. 11. Comparison between model curves and experimental B.T. structure factors in lithium based alloys. By courtesy of Drs. Ruppersberg, Speicher and Reiter.

and Sadoc [25] in their study of amorphous ferromagnetic Co-P alloys by the polarized neutron method. Their results display all the qualitative features of ordered alloys listed below:

- i) large negative value of $A_{PP}(0)$ and superstructure peak at K_S in A_{PP} ,
- ii) large negative superstructure dip at K_S in A_{Co-P} ,
- iii) 'indirect' superstructure bump at K_S in A_{Co-Co} .

However, their precision is too limited for a quantitative interpretation.

Ruppertsberg, Speicher and Reiter's measurements on lithium based alloys [26], [27] are much more accurate and agree almost perfectly with model calculations (see Figure 11). In both Li-Ag [26] and Li-Pb [27] systems, size effects seem to be negligible since the three FFZ structure factors correspond to the same first peak position. Thus $S_{NC}(K) \cong 0$ and the position of S_{CC} superstructure peak at K_S is in good agreement with Equation (28). Furthermore, from the amplitude of S_{CC} oscillations one deduces the following values for the order parameters:

$$\xi = -0.32 \pm 0.05 \text{ or } \eta_{Li-Pb}/\eta_{Li} \cong 0.66 \text{ in Li}_{50}Pb_{50} \text{ alloys}$$

$$\text{and } \xi = -0.24 \pm 0.05 \text{ or } \eta_{Li-Ag}/\eta_{Li} \cong 0.35 \text{ in Li}_{72}Ag_{28} \text{ alloys.}$$

At large K , S_{CC} oscillations are in phase opposition with S_{NN} oscillations in agreement with Equations (25) and (26). Furthermore, it is very likely that the observed oscillation damping could be interpreted if atomic vibrations were taken into account. Such a good agreement between experimental and calculated partial structure factors of binary alloys provides an a posteriori proof for the validity of the model in the pure metal case.

Conclusion

In this paper, we have shown that the structure of liquid metals and alloys may be interpreted in simple geometrical terms. Local chemical ordering in liquid alloys produces large positive or negative values at small K as well as sharp and intense superstructure peaks or dips in the partial structure factors. These modifications with respect to disordered alloys occur before the first peaks of the partial structure factors and may introduce drastic changes in the calculation of transport properties. Furthermore, size difference between alloy components as well as chemical ordering causes the partial structure factors to depend on concentration. Thus, the methods for partial structure factor determination which are based on the assumption of concentration independency are shown to be uncertain.

From a practical point of view, the presence of "prepeaks" in the scattering patterns of a liquid alloy is the sign of local chemical order phenomena. (Thus, it is hopeless to expect a disordered solid solution to be formed by quenching such an alloy from the liquid state). However, careful measurements are needed in order to determine the contribution of each partial structure factor to the total scattering pattern and to derive the mean local neighbourhood of each chemical species.

Acknowledgements

These long numerical calculations were performed on the I.L.L. PDP10 computer with the friendly and efficient cooperation of all operators and computer staff. Mr. S. Claisse is responsible for the careful presentation of the drawings.

Discussions with Drs. P. Chieux, R. Currat, and H. Ruppertsberg were greatly appreciated and special thanks are due to Prof. P. Nozières for his derivation of the equation of state.

I am also indebted to Dr. W. S. Howells for his corrections to the original manuscript.

- [1] J. Blétry, *Z. Naturforsch.* **32a**, 445 (1977).
- [2] A. Guinier, *Théorie et Technique de la Radio cristallographie*, Dunod (1964), p. 452.
- [3] J. D. Bernal, *Proc. Roy. Soc. London A* **280**, 299 (1964).
- [4] L. Landau and E. Lifschitz, *Physique Statistique*, Mir (Moscow 1967).
- [5] J. A. Barker, *Lattice Theories of the Liquid State*, Pergamon (1963).
- [6] J. Blétry, *Z. Naturforsch.* **31a**, 960 (1976).
- [7] A. B. Bhatia and D. E. Thornton, *Phys. Rev. B* **28**, 3004 (1970).
- [8] N. W. Ashcroft and D. C. Langreth, *Phys. Rev.* **156**, 685 (1967).
- [9] G. Fournet, *C. R. Acad. Sci. Paris* **229**, 1071 (1949).
- [10] T. E. Faber and J. M. Ziman, *Phil. Mag.* **11**, 153 (1965).
- [11] J. E. Enderby, D. M. North, and P. A. Egelstaff, *Phil. Mag.* **14**, 961 (1966).
- [12] H. A. Bethe, *Proc. Roy. Soc. London A* **150**, 552 (1935).

- [13] S. Steeb and R. Hezel, *Z. Metallk.* **57**, 374 (1966).
- [14] P. Laty, J. C. Joud, J. C. Mathieu, and P. Desre, To be published in *Phil. Mag.*
- [15] L. Fejes Tóth, *Jber. dtsch. Math. Ver.* **53**, 66 (1934).
- [16] K. Schutte and B. L. van der Waerden, *Math. Annalen* **123**, 96 (1951).
- [17] S. Steeb and H. Entress, *Z. Metallk.* **57**, 803 (1966).
- [18] S. Steeb, H. Dilger, and J. Höhler, *Phys. Chem. Liq.* **1**, 235 (1969).
- [19] H. F. Bühner and S. Steeb, *Z. Metallk.* **62**, 27 (1971).
- [20] A. Boos, S. Steeb, and D. Godel, *Z. Naturforsch.* **27a**, 271 (1972).
- [21] H. Ruppersberg and K. Goebels, *Z. Naturforsch.* **27a**, 1018 (1972).
- [22] S. C. Rowland, S. Narasimhan, and A. Bienenstock, *J. Appl. Phys.* **43**, 2741 (1972).
- [23] F. G. Edwards, J. E. Enderby, R. A. Howe, and D. I. Page, *J. Phys. C* **8**, 3483 (1975).
- [24] D. M. North and C. N. J. Wagner, *Phys. Chem. Liquids* **2**, 87 (1970).
- [25] J. Blétry and J. F. Sadoc, *J. Phys. F* **5**, L110 (1975).
- [26] H. Reiter, H. Ruppersberg, and W. Speicher, 3rd Int. Conf. on Liquid Metals, 133 (Bristol 1976).
- [27] H. Ruppersberg and H. Reiter, private communication.